Physica E 93 (2017) 234–237

Contents lists available at ScienceDirect

Physica E

journal homepage: www.elsevier.com/locate/physe

Study of electronic and optical properties of two-layered hydrogenated aluminum nitrate nanosheet

Somayeh Faghihzadeh, Nasser Shahtahmasebi, Mahmood Rezaee Roknabadi*

Department of Physics, Faculty of Science, Ferdowsi University of Mashhad, Mashhad, Iran

ARTICLE INFO

Keywords:
GW approximation
Optical properties
Self-energy
Dielectric response

ABSTRACT

First principle calculations based on density functional theory using GW approximation and two particle Bethe–Salpeter equation with electron-hole effect were performed to investigate electronic structure and optical properties of two-layered hydrogenated AlN. According to many body green function due to decrease in dimension and considering electron-electron effect, direct (indirect) band gap change from 2 (1.01) eV to 4.83 (3.62) eV. The first peak in imaginary part of dielectric function was observed in parallel direction to a plane obtaining 3.4 was achieved by bound exciton states possess 1.39 eV. The first absorption peak was seen in two parallel and perpendicular directions to a plane which are in UV region.

1. Introduction

Recently, semiconductors and insulators with two dimensional (2D) hexagonal structures have received huge attention due to their particular properties [1–10]. Development of both theoretical and experimental studies on Graphene encouraged researchers to look for new materials. Through these findings, it took great effort into the synthesis of similar structures to graphene such as silicene [11–14], germanene [14–17] and also III-V binary compounds with hexagonal structures [18–22].

Newly, III-V binary compounds are such 2D materials which have become the focus of attention. If carbon atoms in Graphene are substituted with group III and V elements, 2D materials can be formed. Through binary compounds, BN and AlN have received great attention. Studying on AlN revealed that it possess highly chemical stability, excellent mechanical properties and thermal conduction [10,23]. Also AlN because of its semiconducting nature obtaining energy band gap with amount of 6.2 eV through the group III nitrates can be used favorably for nanoelectronic applications [24].

Recently, researchers have shown that it is theoretically and experimentally possible to fabricate 2D nanostructured AlN [25]. It was experimentally reported nanowires [25–28], nanoblelts [29–31] and nanodots [32,33] of AlN were synthetized. Tsipas et al. developed nanosheets of AlN on Ag (1 1 1) surface [10].

Zhang et al. studied the inherited defect of magnetic properties for mono layered AlN and found out structures associated with N showed ferromagnetic property with high Curie point in room temperature [34]. More defects were investigated by others [35]. Studying on such defects indicated that chemical modification can be an effective route in order to control the magnetic and electronic properties of mono layered ALN. In 2015, Xinru Li and his team reported geometric and electronic structures of 2D topological insulators (TIs), g-T1A (A = N, P, As, and Sb) monolayers by first principle calculations. Their calculations showed that g-T1A(A = As, Sb) have large band gap and due to their strong spin orbit coupling can be found as promising 2D TIs.[36].

Recently, 2D hydrogenated planes were observed by researchers [37,38]. It was shown that mono layered or two layered nanoribbons fully or partially hydrogenated such as BN [39], ZnO [40] and AlN [24] depicted intriguing properties. The results indicated that such properties are dependable to wideness and thickness of ribbons and edge modifications. It was reported that doping of some materials by hydrogen makes their energy band gap decreased [41,42]. Therefore hydrogen can have a huge impact on the properties of such materials. It was observed that hydrogenated mono-layered AlN possess lower energy band gap compared to its pristine structure [43]. Zhang et al. [44] works has encouraged us to calculate optical properties of hydrogenated two-layered AlN using Bethe–Salpeter equation in order to introduce electron-hole effect. Many body effects play a key role in electronic and optical properties of low-dimensional systems such as hexagonal mono-layered AlN [45], AlN nanotubes [46] and 2D monolayers [47,48] due to the decrease in screening effects and increase in electron correlation effects. Our first principle calculations revealed that there are great electronic properties and optical response in hydrogenated two-layered AlN associated with graphene. In Section 2 electronic and optical properties of hexagonal two-layered AlN by using Bethe–Salpeter equation and will be discussed. In Section 3 the results of calculations will be analyzed.

* Corresponding author.
E-mail address: roknabad@um.ac.ir (M. Rezaee Roknabadi).

http://dx.doi.org/10.1016/j.physe.2017.03.020
Received 15 September 2016; Received in revised form 4 December 2016; Accepted 27 March 2017
Available online 27 March 2017
1386-9477/

Table 1
Optimized bond lengths of hydrogenated two-layered AlN.

	Lattice constant (Å)	Al-N (Å)	Al-H (Å)	N-H (Å))
LDA[a]	3.03	1.77	1.57	1.03
GGA[b]	3.11	1.83	1.58	1.029

[a] Present calculation.
[b] Ref. [44]

2. Computational methods

Our calculations were performed using DFT and the quantum espresso software package [49] which uses norm-conserving pseudo-potential [50] in order to obtain ground-state electronic properties of hydrogenated two-layered AlN. For the exchange and correlation terms, the local density approximation with parameter of Pedrew-Zunger [51] has been used. For charge density and pseudo-wave-functions were expanded by plane waves with a cutoff energy equal to 80 Ry and 400 Ry. The Brillouin zone has been sampled using 18×18×1 Monkhorst-Pack k-point grids [52]. All the coordinates of the atoms were relaxed until the Hellman–Feynman forces were less than 0.02 eV/Å for the entire geometry optimization. The lattice constant was calculated to be 3.03 Å which is in good agreement with others [44]. AlN includes a 2D hydrogenated two-layered plane. We carried out calculation with the periodicity along x-y axis and the separation between planes along z axis was set to be 18 Å to make sure that they do not interact with each other. The optimized bond length amounts of AlN after relaxation are shown in Table 1. Fig. 1. Presents the top and side view of relaxed hydrogenated two-layered AlN. To investigate the dynamic stability, we performed phonon calculations and understood that there is not an instability related with a phonon mode with K in BZ. We have considered the results shown in the Fig. 2. By considering ground-state, the electron-electron effects can be introduced via G_0W_0 approximation (The calculations were performed in none non-self-consistent) and self-energy term to obtain the energies of quasiparticles. The energy can be calculated in GW approximation from relations bellow:

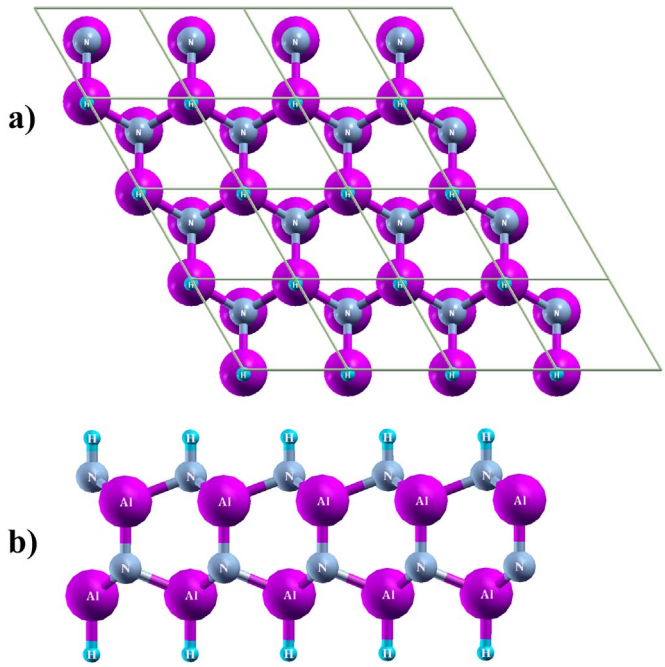

Fig. 1. Top (a) and side views (b) of the relaxed hydrogenated two-layered AlN structure.

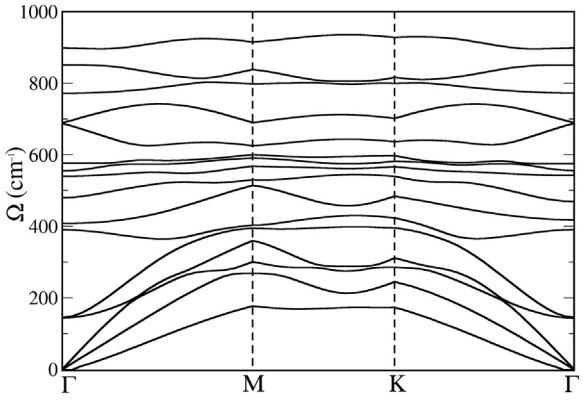

Fig. 2. Calculated vibration frequencies of phonon modes Ω versus k of hydrogenated two-layered AlN.

$$E_{\mathbf{nk}}^{QP} = \varepsilon_{\mathbf{nk}}^{KS} + Z_{\mathbf{nk}}(\varepsilon_{\mathbf{nk}}^{KS})\langle\psi_{\mathbf{nk}}|\sum(\varepsilon_{\mathbf{nk}}^{KS}) - V_{xc}^{LDA}\|\psi_{\mathbf{nk}}\rangle,$$
$$Z_{\mathbf{nk}}(\varepsilon_{\mathbf{nk}}^{KS}) = \left[1 - \partial\sum/\partial E|_{\varepsilon_{\mathbf{nk}}^{KS}}\right]^{-1} \quad (1)$$

where Z_{nk} is a normal factor. In order to determine exchange-correlation potential, the local density approximation term was used. The self-energy $\sum$ can be calculated by GW approximation [53,54]:

$$\sum = iGW \quad (2)$$

where G is the one-particle green's function and W is the screened coulomb interaction. The electron-hole effects can be considered after obtaining the energies of quasiparticles. The electron-electron and electron-hole effects can be calculated using yambo code [55]. Finally by solving the Bethe–Salpeter equation, the effects mentioned can be introduced into calculations [53,56].

$$(E_{ck} - E_{ck})A_{vck}^{S} + \sum_{k'v'c'}\langle vck|K^{d} + 2K^{x}|v'c'k'\rangle = \Omega^{S}A_{vck}^{S} \quad (3)$$

In equation above, E_{ck} and E_{vk} are energies of quasiparticles for conduction and valence bonds, respectively. Ω^S and A^S are eigen values and eigen functions. K^d is related to screened coulomb interaction. GW and Bethe–Salpeter calculations in terms of number of bands, energy cutoff and number of K are well convergent. In our calculations, amounts of 400 bands for expanding Green function, 10000 wave vectors for exchange term and 400 wave vectors for self-energy correlation were implemented. The optical absorption spectra was obtained by including amounts of 9 valence bonds and 6 conduction bonds when applied electric field is along x-z direction. It must note that a reason for optioning such numbers is that optical spectra and energies of quasiparticles were favorably convergent in this state, i.e. the optical spectra and energy of a quasiparticle remain constant. In GW and BSE calculations, the coulomb interaction along direction which is perpendicular to two-layered plane, in amount of 40 Bohr was truncated [57]. In two-particle Hamiltonian we have used Tamm-Dankov approximation [53,54].

3. Results and discussion

By considering electron-electron effects, band structure of optimized two-layered structure using LDA and GW approximation can be seen in Fig. 3. By taking LDA, amounts of direct and indirect band gap were observed in Γ and Γ–K points 2.21 eV and 1.01 eV, respectively [44]. By taking self-energy corrections amounts of direct and indirect band gap were increased to 4.83 eV and 3.62 eV, respectively. It also reported the amount of the energy band gap for non-hydrogenated mono-layered AlN was calculated to be 5.36 eV using GW+LDA [45].

Several works indicated that using calculations with GW approximation made the energy band gap theoretically modified compared to

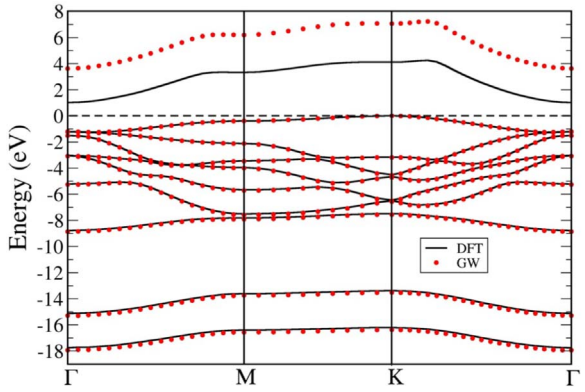

Fig. 3. Electronic band structures of the hydrogenated two-layered AlN structure. The black lines and the red circles in the band structures depict at DFT and GW calculations, respectively. The Fermi level is set to zero. (For interpretation of the references to color in this figure legend, the reader is referred to the web version of this article.)

experimental values [55,58]. In our two-layered structure by implementing quasiparticles corrections, the energy band gap using DFT +LDA is increased to be 3.56 eV compared to GW+LDA approximation. The increase in energy band gap is due to decrease in effective electronic screening cause coulomb interaction to be enhanced. The results of calculations with GW compared to DFT remarked that electron-electron effects for two-layered structure have an effect on conduction bands which is ineffective that of valence bands. Generally the DFT (LDA or GGA) has some limitations for excited states and conduction bands. The theories beyond DFT mostly modify the conduction bands, but affect on both the valence and conduction bands for some materials [59]. Our results showed that the GW calculations only have influence on conduction band, while have little effect on valance band. This results is in a good agreement with some previous theoretical results [45,60,61].

Therefore the amount of energy in conduction bands of DFT approximation is corresponded to that of GW if it is shifted to be 2.64 eV.

Fig. 4. shows real and imaginary part of dielectric function in terms of incident photon energy along x and y directions by using GW+BSE and GW+RPA calculations. The real and imaginary parts of dielectric function along x axis are shown by black lines whereas these parts along y axis using GW+BSE are depicted by black points in Fig. 4, a and b. Also red lines and red points are indicator of dielectric function with GW+RPA calculations. Fig. 4. shows that two spectra along x and y direction are well matched with each other which implies that two-layered structure along x and y direction is isotropic. This result shows good agreement with 2D materials [59,62–64]. In GW+RPA calculations electron-electron effects were considered, although in GW+BSE calculations both electron-electron and electron-hole effects are implemented. In both directions, when self-energy correction is used, all spectra move to higher energies (blue shift). When electron-hole interaction effects are considered, all spectra move backward reversely. Therefore removal of band gap broadened is indicative of quasiparticle correction and change in optical absorption is due to the exciton effects.

Fig. 5. shows dielectric function in terms of incident photon energy along x and z directions. By comparing both spectra it can be found out the structure is non-isotropic. By comparing optical absorption in z and x directions, it can be understood in amount of energies lover than 13 eV, absorption in x direction is more than z direction. This state is inversed in amount of energies higher than 13 eV. More absorption in lower energies along x and y compared to z direction implies that structure is periodic along x and y direction whereas in z direction is limited. As shown in Fig. 5. the first absorption peak (bright exciton) is observed in range of 3.4 eV in x direction. This value is in the range of 3.5 eV along z direction. In both directions, the first absorption peak is located in UV region. As seen in Fig. 5. the first peak in x and z

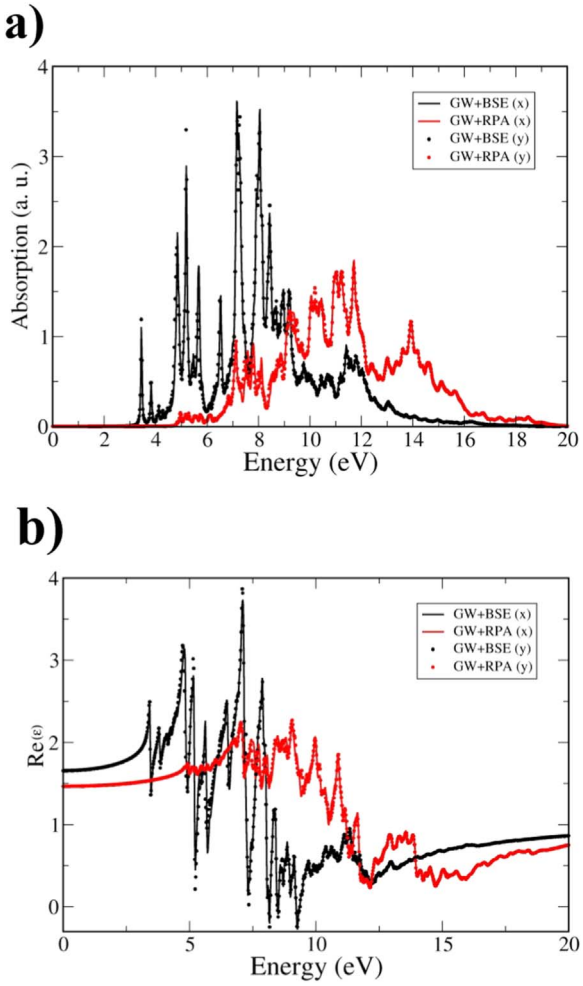

Fig. 4. (a) Imaginary part and (b) Real part of dielectric function. The optical spectrum for light polarized parallel to the hydrogenated two-layered AlN calculated with (black line and circles) and without (red line and circles) consideration of the electron-hole interactions, i.e., GW + BSE and GW + RPA, respectively. (For interpretation of the references to color in this figure legend, the reader is referred to the web version of this article.)

directions are close to each other because when layers are increased in z direction, the structure becomes rather bulk which causes absorption peak in z direction to move toward x direction. The binding energy of the first exciton along x direction is calculated to be 1.39 eV. Due to band structure of material and considering GW+BSE calculations, the most significant contribution about absorption peak along x direction is related to numbers of 8th and 9th bands transition into 10th band. The numbers of energy intervals (shown in Fig. 5(a)) which cause dielectric function to be zero (i.e. electromagnetic wave cannot be propagated in these intervals) are more in amounts of energy lower than 13 eV along x direction than that of z direction. Spatially, despite of x direction in lower energies, there is no real root in z direction for real part of dielectric function.

4. Conclusion

In this paper, optical properties of hydrogenated two-layered AlN using BSE method associated with quasiparticle (QP) corrections in GW approximation were studied. GW calculations showed that the electron-electron effects have a significant effect on the band structure of AlN, so it can modifies the band gap to the amounts of 2.61 eV. The two-layered structure is isotropic along x and y direction, but non-isotropic in z direction. The first absorption peak is shown along parallel and perpendicular to the plane by using GW+BSE calculations

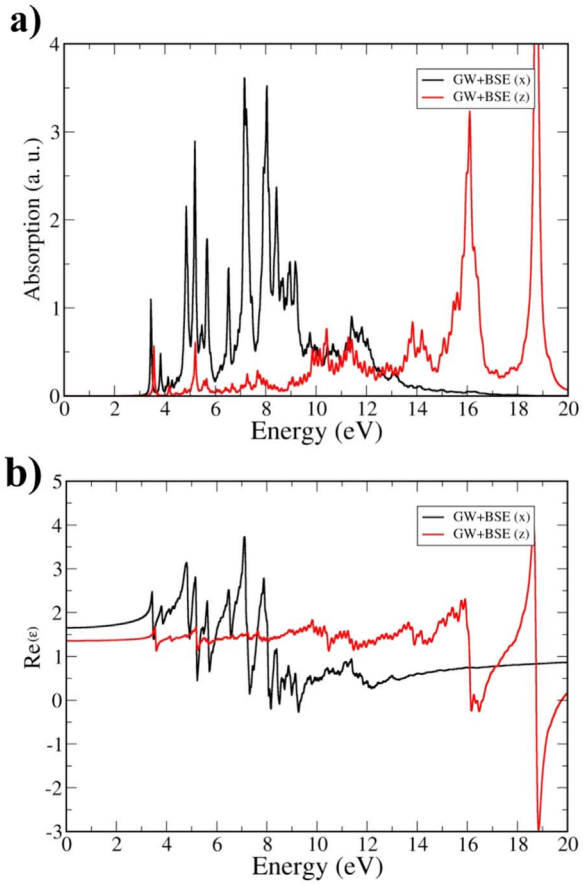

Fig. 5. (a) Imaginary part and (b) Real part of dielectric function. The optical spectrum for light polarized parallel (black line) and perpendicular (red line) to the hydrogenated two-layered AlN calculated with consideration of the electron-hole interactions. (For interpretation of the references to color in this figure legend, the reader is referred to the web version of this article.)

are 3.44 eV and 3.5 eV in UV region, respectively. Therefore it is expected that structures based AlN exhibit remarkable properties, which plays an important role in nanoelectronic industry.

References

[1] K. Li, X.B. Du, Y. Yan, H.X. Wang, Q. Zhan, H.M. Jin, Phys. Lett. A 374 (2010) 3671.
[2] X.Y. Peng, R. Ahuja, Appl. Phys. Lett. 94 (2009) 102504.
[3] R.L. Han, W. Yuan, H. Yang, X.B. Du, Y. Yan, H.M. Jin, J. Magn. Magn. Mater. 326 (2013) 45.
[4] X. Zhang, Z. Liu, S. Hark, Solid State Commun. 143 (2007) 317.
[5] J. Pastrnak, A.N. Trukhin, Czech, J. Phys. Sect. B 27 (1977) 715.
[6] P. Liu, A.D. Sarkar, R. Ahuja, Comput. Mater. Sci. 86 (2014) 206.
[7] C.W. Zhang, J. Appl. Phys. 111 (2012) 043702.
[8] E.F. de Almeida Junior, F. de Brito Mota, C.M.C. de Castilho, A. Kakanakova-Georgieva, G.K. Gueorguiev, Eur. Phys. J. B 85 (2012) 48.
[9] Q. Wu, Z. Hu, X.Z. Wang, Y.M. Hu, Y.J. Tian, Y. Chen, Diam. Relat. Mater. 13 (2004) 38.
[10] P. Tsipas, et al., Appl. Phys. Lett. 103 (2013) 251605.
[11] A. Kara, H. Enriquez, A.P. Seitsonen, L.C.L.Y. Voon, S. Vizzini, B. Aufray, Hamid Oughaddou, Surf. Sci. Rep. 67 (2012) 1.
[12] H. Liu, J. Gao, J. Zhao, J. Phys. Chem. C. 10353 (2013) 117.
[13] H. Sahin, J. Sivek, S. Li, B. Partoens, F.M. Peeters, Phys. Rev. B 88 (2013) 045434.
[14] S. Cahangirov, M. Topsakal, E. Akturk, H. Sahin, S. Ciraci, Phys. Rev. Lett. 102 (2009) 236804.
[15] Z. Ni, Q. Liu, K. Tang, J. Zheng, J. Zhou, R.Q.Z. Gao, D. Yu, J. Lu, Nano Lett. 113 (2012) 12.
[16] M.E. Davila, L. Xian, S. Cahangirov, A. Rubio, G. Le Lay, New J. Phys. 16 (2014) 095002.
[17] K. Yang, S. Cahangirov, A. Cantarero, A. Rubio, R. D' Agosta, Phys. Rev. B 89 (2014) 125403.
[18] H.L. Zhuang, R.G. Hennig, Appl. Phys. Lett. 101 (2012) 153109.
[19] Q. Wang, Q. Sun, P. Jena, Y. Kawazoe, ACS Nano 3 (2009) 621.
[20] K.K. Kim, A. Hsu, X. Jia, S.M. Kim, Y. Shi, M. Hofmann, D. Nezich, J.F. Rodriguez-Nieva, M. Dresselhaus, T. Palacios, J. Kong, Nano Lett. 12 (2012) 16.
[21] M. Farahani, T.S. Ahmadi, A. Seif, J. Mol. Struct. 913 (2009) 126.
[22] H. Sahin, S. Cahangirov, M. Topsakal, E. Bekaroglu, E. Akturk, R.T. Senger, S. Ciraci, Phys. Rev. B 80 (2009) 155453.
[23] Y. Taniyasu, M. Kasu, Appl. Phys. Lett. 98 (2011) 131910.
[24] A.J. Du, Z.H. Zhu, Y. Chen, G.Q. Lu, Sean Smith, Chem. Phys. Lett. 469 (2009) 183.
[25] Q. Wu, Z. Hu, X.Z. Wang, Y.M. Hu, Y.J. Tian, Y. Chen, Diam. Relat. Mater. 13 (2004) 38.
[26] J.H. Duan, S.G. Yang, H.W. Liu, J.F. Gong, H.B. Guang, X.N. Zhao, R. Zhang, Y.W. Du, J. Phys. Chem. B 109 (2005) 3701.
[27] Q. Zhao, H.Z. Zhang, X.Y. Xu, Z. Wang, J. Xu, D.P. Yu, G.H. Li, F.H. Su, Appl. Phys. Lett. 86 (2005) 193101.
[28] Y. Li, J. Xiang, F. Qian, S. Gradecak, Y. Wu, H. Yan, H. Yan, D.A. Blom, C.M. Lieber, Nano Lett. 6 (2006) 1468.
[29] Q. Wu, Z. Hu, X.Z. Wang, Y. Chen, Y. Lu, J. Phys. Chem. B 107 (2003) 9726.
[30] Y.B. Tang, H.T. Cong, F. Li, H.M. Cheng, Diam. Relat. Mater. 16 (2007) 537.
[31] L.S. Yu, Y.Y. Lv, X.L. Zhang, Y.Y. Zhang, R.Y. Zou, F. Zhang, J. Cryst. Growth 334 (2011) 57.
[32] W.H. Goh, et al., J. Cryst. Growth 315 (2011) 160.
[33] Z. Bouchkour, P. Tristant, E. Thune, C. Dublanche-Tixier, C. Jaoul, R. Guinebretiere, Surf. Coat. Technol. 205 (2011) 586.
[34] C.W. Zhang, J. Appl. Phys. 111 (2012) 043702.
[35] E.F. de Almeida Junior, F. de Brito Mota, C.M.C. de Castilho, A. Kakanakova-Georgieva, G.K. Gueorguiev, Eur. Phys. J. B 85 (2012) 48.
[36] X. Li, Y. Dai, Y. Ma, W. Wei, L. Yu, B. Huang, Nano Res. 8 (2015) 2954–2962.
[37] D.C. Elias, et al., Science 323 (2009) 610.
[38] S. Ryu, M.Y. Han, J. Maultzsch, T.F. Heinz, P. Kim, M.L. Steigerwald, L.E. Brus, Nano Lett. 8 (2008) 4597.
[39] W. Chen, Y. Li, G. Yu, C. Li, S.B. Zhang, Z. Zhou, Z. Chen, J. Am. Chem. Soc. 132 (2010) 1699.
[40] L. Kou, C. Li, Z. Zhang, W. Guo, ACS Nano 4 (2010) 2124.
[41] F.W. Averill, J.R. Morris, V.R. Cooper, Phys. Rev. B 80 (2009) 195411.
[42] Y. Wang, Phys Status Solidi-Rapid, Res. Lett. 4 (2010) 34.
[43] C. Zhang, F. Zheng, J. Comput. Chem. 32 (2011) 3122.
[44] W. Zhang, T. Li, S.G. Gong, C. He, L. Duan, Phys. Chem. Chem. Phys. 17 (2015) 10919.
[45] D. Vahedi Fakhrabad, N. Shahtahmasebi, M. Ashhadi, Superlattices Microstruct. 79 (2015) 38.
[46] K. Rezouali, M.A. Belkhir, A. Houari, J. Bai, Comp. Mater. Sci. 45 (2) (2009) 305.
[47] G. Luo, X. Qian, H. Liu, R. Qin, J. Zhou, L. Li, Z. Gao, E. Wang, W.N. Mei, J. Lu, Y. Li, S. Nagase, Phys. Rev. B 84 (2011) 075439.
[48] D. Prezzi, D. Varsano, A. Ruini, A. Marini, E. Molinari, Phys. Rev. B 77 (2008) 041404.
[49] P. Giannozzi, et al., J. Phys.: Condens. Matter 21 (2009) 395502.
[50] N. Troullier, J.L. Martins, Phys. Rev. B 43 (1991) 1993.
[51] J.P. Perdew, A. Zunger, Phys. Rev. B 23 (1981) 5048.
[52] H.J. Monkhorst, J.D. Pack, Phys. Rev. B 13 (1976) 5188.
[53] M. Rohlfing, S.G. Louie, Phys. Rev. B 62 (2000) 4927.
[54] G. Onida, L. Reining, A. Rubio, Rev. Mod. Phys. 74 (2002) 601.
[55] A. Marini, C. Hogan, M. Gruning, D. Varsano, Comput. Phys. Commun. 180 (2009) 1392.
[56] G. Strinati, Phys. Rev. B 29 (1984) 5718.
[57] C.A. Rozzi, D. Varsano, A. Marini, E.K.U. Gross, A. Rubio, Phys. Rev. B 73 (2006) 205119.
[58] G. Luo, X. Qian, H. Liu, R. Qin, J. Zhou, L. Li, et al., Phys. Rev. B 84 (2011) 075439.
[59] W. Wei, Y. Dai, B. Huanga, T. Jacob, Phys. Chem. Chem. Phys. 15 (2013) 8789.
[60] P. Rinke, A. Qteish, J. Neugebauer, C. Freysoldt, M. Scheffler, New J. Physics7 (2005) 126.
[61] W. Wei, Y. Dai, B. Huang, T. Jacob, J. Chem. Phys. 139 (2013) 144703.
[62] W. Wei, Y. Dai, B. Huang, T. Jacob, J. Chem. Phys. 139 (2013) 144703.
[63] W. Wei, T. Jacob, Phys. Rev. B 88 (2013) 045203.
[64] C. Attaccalite, M. Bockstedte, A. Marini, A. Rubio, L. Wirtz, Phys. Rev. B 83 (2011) 144115.